Heliyon 9 (2023) e15587

Contents lists available at ScienceDirect

Heliyon

journal homepage: www.cell.com/heliyon

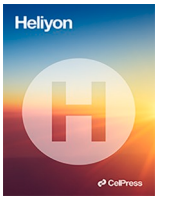

Research article

Broadly neutralizing antibodies against Omicron variants of SARS-CoV-2 derived from mRNA-lipid nanoparticle-immunized mice

Ruei-Min Lu [a], Kang-Hao Liang [a], Hsiao-Ling Chiang [a], Fu-Fei Hsu [a], Hsiu-Ting Lin [b], Wan-Yu Chen [b], Feng-Yi Ke [a], Monika Kumari [b], Yu-Chi Chou [a], Mi-Hua Tao [a,c], Yi-Ling Lin [a,c], Han-Chung Wu [a,b,*]

[a] Biomedical Translation Research Center (BioTReC), Academia Sinica, Taipei, Taiwan
[b] Institute of Cellular and Organismic Biology (ICOB), Academia Sinica, Taipei, Taiwan
[c] Institute of Biomedical Sciences (IBMS), Academia Sinica, Taipei, Taiwan

ARTICLE INFO

Keywords:
SARS-CoV-2
COVID-19
mRNA LNP
Antibody humanization
Neutralizing antibody

ABSTRACT

The COVID-19 pandemic continues to threaten human health worldwide as new variants of the severe acute respiratory syndrome coronavirus 2 (SARS-CoV-2) emerge. Currently, the predominant circulating strains around the world are Omicron variants, which can evade many therapeutic antibodies. Thus, the development of new broadly neutralizing antibodies remains an urgent need. In this work, we address this need by using the mRNA-lipid nanoparticle immunization method to generate a set of Omicron-targeting monoclonal antibodies. Five of our novel K-RBD-mAbs show strong binding and neutralizing activities toward all SARS-CoV-2 variants of concern (Alpha, Beta, Gamma, Delta and Omicron). Notably, the epitopes of these five K-RBD-mAbs are overlapping and localized around Y453 and F486 of the spike protein receptor binding domain (RBD). Chimeric derivatives of the five antibodies (K-RBD-chAbs) neutralize Omicron sublineages BA.1 and BA.2 with low IC_{50} values ranging from 5.7 to 12.9 ng/mL. Additionally, we performed antibody humanization on broadly neutralizing chimeric antibodies to create K-RBD-hAb-60 and -62, which still retain excellent neutralizing activity against Omicron. Our results collectively suggest that these five therapeutic antibodies may effectively combat current and emerging SARS-CoV-2 variants, including Omicron BA.1 and BA.2. Therefore, the antibodies can potentially be used as universal neutralizing antibodies against SARS-CoV-2.

1. Introduction

According to World Health Organization (WHO) reports through December 2022, over 641 million people have been infected and 6.62 million have died as a result of the worldwide coronavirus disease 2019 (COVID-19) pandemic. The causal pathogen, severe acute respiratory syndrome coronavirus 2 (SARS-CoV-2), is a betacoronavirus with a linear single-stranded, positive-sense RNA genome (~30 kb) encoding 29 proteins [1]. SARS-CoV-2 infection is mediated by its spike protein, which is composed of an S2 domain and an

* Corresponding author. Institute of Cellular and Organismic Biology, Academia Sinica No. 128, Academia Road, Section 2, Nankang, Taipei 11529, Taiwan.
E-mail address: hcw0928@gate.sinica.edu.tw (H.-C. Wu).

https://doi.org/10.1016/j.heliyon.2023.e15587
Received 10 August 2022; Received in revised form 7 April 2023; Accepted 14 April 2023
Available online 18 April 2023

S1 domain that contains an N-terminal domain (NTD), a C-terminal domain (CTD), and a receptor binding domain (RBD) [2]. The RBD is an especially critical domain, as it initiates viral entry into host cells upon its binding to the host-cell receptor, angiotensin-converting enzyme 2 (ACE2). Due to its crucial role in infection, the RBD has been a common target for novel vaccines and neutralizing antibodies.

The high mutation rate associated with SARS-CoV-2 has contributed to its rapid global transmission, with many variants arising since the initial outbreak in late December 2019 [3]. Some of these variants are highly transmissible and can evade neutralization by vaccine-induced and therapeutic antibodies. Thus, the WHO has designated several "variants of concern" (VOCs), including Alpha (B.1.1.7), Beta (B.1.351), Gamma (P.1), Delta (B.617.2) and Omicron (B.1.1.529) [4]. Beta carries three mutations in the RBD (K417N, E484K and N501Y) and was found to effectively evade immune response and neutralizing antibodies [5]. The Alpha variant became dominant globally in early 2021 due to its high transmissibility compared to previous lineages [6]. In the third quarter of 2021, Alpha was gradually replaced by Delta, which exhibits even greater infectivity and pathogenicity, along with an ability to evade some neutralizing antibodies [7, 8].

On November 24, 2021, Omicron was first reported in South Africa, and two days later, WHO classified it as the fifth VOC. After just one month, Omicron had already outcompeted Delta to become the dominant circulating variant around the world; this rapid change is mainly due to the remarkably short caseload doubling time (2–3 days) [9, 10]. As of June 2022, the Omicron variant has diverged into five distinct sublineages: BA.1, BA.2, BA.3, BA.4 and BA.5 [11]. In the first half of 2022, the most common circulating Omicron sublineage is BA.2. Compared to the original Wuhan-Hu-1 strain, Omicron BA.2 carries at least 30 mutations in the spike protein (28 amino acid substitutions and three small deletions), 16 of which are in the RBD. Eight of the 16 amino acid alterations in the RBD are located within the receptor-binding motif (RBM), which comprises the major site of contact with the human ACE2 receptor. The mutations in the RBM include: N440K, S477N, T478K, E484A, Q493R, Q498R, N501Y and Y505H. Together, these mutations increase the binding affinity of Omicron RBD to ACE2 by 2.4-fold and render the Omicron variants much more infectious than the Delta variant [11]. Since the RBD is the primary target of neutralizing antibodies induced by COVID-19 vaccines, the accumulation of numerous mutations in this region has strongly reduced the affinity of vaccine-induced neutralizing antibodies, greatly weakening vaccine efficacy. Several studies have demonstrated that the current COVID-19 vaccines (i.e., mRNA-1273, BNT16b2, ChAdOx1 nCoV-19 and Ad26.COV2.S) have substantially reduced neutralizing potencies against Omicron, even in fully vaccinated individuals [11, 12, 13, 14].

Monoclonal antibodies (mAbs) have been widely used in basic research and clinical practice because of their high specificity and versatility [15]. Such properties also make mAbs highly useful in the rapid development of antibody drugs and diagnostic kits to fight COVID-19 [4]. Over the past two years, several neutralizing mAbs have shown *in vivo* efficacy for the prevention and treatment of SARS-CoV-2 [17,18]. For example, REGN-COV2 (combination of casirivimab and imdevimab) reduced the risk of COVID-19-related hospitalization and death by 70% in a cohort of non-hospitalized patients [16]. REGN-COV2 was also able to prevent symptomatic COVID-19 and asymptomatic SARS-CoV-2 infection in previously uninfected household contacts of infected persons [17]. Another neutralizing mAb treatment, AZD7442 (combination of tixagevimab and cilgavimab), caused a statistically significant reduction in the risk of developing symptomatic COVID-19, with protection from the virus continuing for at least 6 months [18]. Altogether, the sustained efforts of researchers in academia and industry have so far yielded eight mAbs with emergency use authorizations (EUAs) granted by the U.S. FDA; these approved mAbs include: bamlanivimab, etesevimab, casirivimab, imdevimab, sotrovimab, cilgavimab, tixagevimab and bebtelovimab [19, 20, 21, 22, 23, 24]. Unfortunately, pseudovirus and authentic virus experiments have shown that Omicron BA.1 is entirely resistant to bamlanivimab, etesevimab, casirivimab and imdevimab ($IC_{50} > 10$ μg/mL), and it is partially resistant to sotrovimab, cilgavimab and tixagevimab ($1 > IC_{50} > 0.1$ μg/mL) [11, 12, 13, 25, 26, 27, 28]. Only bebtelovimab retains high neutralizing activity toward Omicron BA.1 ($IC_{50} < 0.01$ μg/mL) [24]. According to a recent study published in *Nature*, Omicron BA.1 can escape over 85% of 247 anti-RBD neutralizing antibodies in clinical use or under development [25].

In our previous work, we generated six chimeric neutralizing antibodies against the RBD of SARS-CoV-2 spike protein [29]. We showed that cocktails of these antibodies can neutralize D614G, Epsilon (B.1.429) and Kappa (B.1.617.1) strains, as well as four VOCs (Alpha, Beta, Gamma and Delta). The prophylactic and therapeutic activities of the individual neutralizing antibodies or antibody cocktails were then confirmed in D614G- and Delta-variant-infected mouse and hamster models [30]. Although antibody therapy was effective in neutralizing the relevant VOCs of the time, we later found that Omicron BA.1 appears to be refractory to neutralization by our six mAbs. Since nearly all of the commercially available mAbs mentioned above are also ineffective against Omicron, there remains an unmet need for therapeutic antibodies with high neutralizing potency toward currently dominant variants. To quickly identify neutralizing antibodies for Omicron variants, we began by immunizing mice with messenger RNA (mRNA) encapsulated in lipid nanoparticles (LNPs), mimicking the now widely applied vaccine strategy. LNP-mediated delivery is a key aspect of the successful implementation of mRNA-based vaccines; BNT162b2 and mRNA-1273 each show >94% efficacy for preventing COVID-19 and have received EUAs in many countries [31, 32, 33]. In our recent work, we established a platform that combines the mRNA-LNP immunization and hybridoma approaches, and we used it to rapidly generate neutralizing antibodies against the SARS-CoV-2 Delta variant [34]. This time-saving method does not require manufacture of proteins as antigens, as the target protein is directly expressed in the animal and efficiently stimulates humoral immunity. In this study, we utilized bivalent mRNA-LNP encoding spike protein and the RBD of the Kappa variant to generate mAbs. The resulting mAbs were then screened for the ability to neutralize Omicron BA.1 and BA.2 pseudoviruses. Five of the most active anti-Omicron neutralizing antibodies were then engineered into chimeric formats and two were further humanized to enhance the potential for future use of these reagents in clinical settings.

2. Materials and methods

2.1. Generation of mAbs using mRNA-LNP immunization method

Anti-Kappa RBD mAbs were generated according to our previously published procedure [34]. Briefly, an *in vitro* transcription system was used to generate mRNA encoding full-length spike and RBD of the SARS-CoV-2 Kappa variant (QTZ19256.1); the mRNA also contained a 5' UTR, IgG kappa leader sequence, 3' UTR and poly(A) tail. Individual lipids were dissolved in ethanol and mixed. DLin-MC3-DMA (MC3) (MedChemExpress), 1, 2-distearoyl-sn-glycero-3-phosphocholine (DSPC) (Avanti Polar Lipids), cholesterol (Sigma-Aldrich) and PEG-2000 (MedChemExpress) were combined at molar ratios of 50:10:38.5:1.5. The lipid mixture was then combined with a 50 mM sodium acetate buffer pH 4.5, containing mRNA at a ratio of 3:1 (aqueous: ethanol), prior to mixing in NanoAssemblr® IGNITE NxGen Cartridges (Precision NanoSystems Inc.). After formulation, LNPs were dialyzed against PBS (pH 7.4) and concentrated using Amicon Ultra-Centrifugal Filter with a 10-kDa cutoff (Merck).

Four-to six-week-old female BALB/c mice were immunized with 5 μg of the Kappa spike and RBD mRNA-LNP by intramuscular (I.M.) injection. After four inoculations with the same concentration of mRNA-LNP, the splenocytes from immunized mice were harvested and fused with mouse myeloma NS-1 cells. The fused cells were cultured in DMEM supplemented with 15% FBS, HAT medium, and hybridoma cloning factors in 96-well tissue culture plates [35]. Two weeks after fusion, the culture supernatants were screened by ELISA. Selected clones were subcloned via limiting dilutions. Hybridoma clones were isotyped using a commercially available ELISA isotyping it (Southern Biotech, Birmingham, AL, USA). All animal experiments were approved by the Academia Sinica Institutional Animal Care and Use Committee (IACUC protocol No. 20051468).

3. Recombinant protein-based ELISA

Recombinant RBD and spike-His tag proteins for different SARS-CoV-2 variants were purchased from ACROBiosystems. ELISA plates were coated with 0.5 μg/mL recombinant protein in 0.1 M $NaHCO_3$ (pH 8.6) buffer at 4 °C overnight, followed by blocking with PBS containing 1% bovine serum albumin (BSA) at room temperature for 2 h. After blocking, the wells were washed twice with PBS. Anti-RBD and control antibodies were added to the plates and incubated for 1 h at room temperature. The plates were washed with PBS containing 0.1% Tween-20 ($PBST_{0.1}$) three times and then incubated for 1 h with Peroxidase-conjugated secondary antibody (Jackson ImmunoResearch). After three washes with $PBST_{0.1}$, signal was produced using 3,3'5,5'-Tetramethylbenzidine (TMB) substrate (TMBW-1000-01, SURMODICS). The reaction was stopped with 3 N HCl, and absorbance was measured at 450 nm with an ELISA plate reader.

3.1. Pseudovirus neutralization assay

Pseudovirus expressing SARS-CoV-2 spike protein was provided by the National RNAi Core Facility (Academia Sinica, Taiwan). The pseudovirus neutralization assays were performed using HEK293T cells that expressed human ACE2 (HEK293T/hACE2) seeded on 96-well white plates (SPL Life Science) at a density of 1×10^4 cells per well. Serial dilutions of K-RBD-mAbs were pre-incubated with 1000 TU SARS-CoV-2 pseudovirus in 1% FBS DMEM for 1 h at 37 °C. The mixtures were then added to pre-seeded HEK293T/hACE2 cells for 24 h at 37 °C. The pseudovirus-containing culture medium was removed and replaced with 10% FBS DMEM for an additional 48-h incubation. Next, ONE-Glo luciferase reagent (Promega) was added to each well for a 3-min incubation at 37 °C. The luminescence was measured with a microplate spectrophotometer (ID3, Molecular Devices). The half maximal inhibitory concentration (IC_{50}) was calculated by nonlinear regression using Prism software version 8.1.0 (GraphPad Software Inc.).

4. Identification of V_H and V_K sequence of mAbs

Total RNA was extracted from hybridoma cells using TRIzol reagent (Thermo Scientific), and cDNA was generated with an oligo $(dT)_{20}$ primer and Superscript III reverse transcriptase (Thermo Scientific). The V_H and V_L gene fragments were amplified from the cDNA by PCR using primer sets directed against the mouse immunoglobulin (Ig) variable region [36]. The PCR products were cloned using the pGEM-T Easy Vector System (Promega) and analyzed by DNA sequencing. From the sequences, the framework regions (FRs) and complementarity determining regions (CDRs) were defined by searching with the NCBI IgBLAST program (https://www.ncbi.nlm.nih.gov/igblast/).

4.1. Cellular ELISA

The binding of K-RBD-mAbs to the RBD mutants was examined by cellular ELISA. Human HEK293T cells were transiently transfected in 6-well plates with wild-type or mutant RBD plasmids. The next day, transfected cells were seeded on 96-well plates. The cells were fixed with 4% paraformaldehyde in PBS for 15 min at room temperature at 48 h post-transfection and then incubated in 0.1% Triton X-100 at room temperature for 10 min. After blocking the cells with 5% milk, antibodies against RBD were added to the wells (100 ng/mL) for 1 h at room temperature. Then, the cells were washed and horseradish peroxidase-conjugated anti-human antibody (1:2000) was added for 1 h at room temperature. Signal was generated with TMB and was measured on an ELISA plate reader.

Table 1
Characterization of the mAbs activities against RBD of SARS-CoV-2.

	ELISA Binding Activities*					Neutralizing Activities**						
	Wuhan RBD	Kappa RBD	Delta RBD	Omicron BA.1 RBD	Omicron BA.1 spike	Alpha	Beta	Gamma	Kappa	Delta	Omicron BA.1	Isotype
K-RBD-mAb-1	+ + +	+ + +	+ +	+ +	-	+	+	+	n.d.	+ +	n.d.	IgG2a; k
K-RBD-mAb-3	+ + +	+ + +	+ +	+	-	-	-	-	n.d.	-	n.d.	IgG2a; k
K-RBD-mAb-5	+ + +	+ + +	+ + +	+ +	+ +	+	-	+	n.d.	-	-	IgG2a; k
K-RBD-mAb-7	+ + +	+ + +	+ + +	+	-	+	+	+	n.d.	+	n.d.	IgG2b; k
K-RBD-mAb-11	+ + +	+ + +	+ + +	+ + +	+	-	-	-	n.d.	-	-	IgG2b; k
K-RBD-mAb-13	+ + +	+ + +	+ +	-	-	-	-	-	n.d.	-	n.d.	IgG1; k
K-RBD-mAb-14	+ + +	+ + +	+ + +	-	-	+	+	+	n.d.	+	n.d.	IgG1; k
K-RBD-mAb-18	+ +	+ + +	+ + +	+	-	-	-	-	n.d.	-	n.d.	IgG2a; k
K-RBD-mAb-22	+ + +	+ + +	+ + +	-	-	+	+	+	n.d.	+	n.d.	IgG2a; k
K-RBD-mAb-23	+ + +	+ + +	+ + +	+ +	+	-	-	-	n.d.	-	-	IgG2b; k
K-RBD-mAb-26	+ + +	+ + +	+ + +	-	-	+	+	+	n.d.	+	n.d.	IgG1; k
K-RBD-mAb-31	+ +	+ + +	-	+	-	n.d.	n.d.	n.d.	n.d.	n.d.	n.d.	IgG2a; k
K-RBD-mAb-32	+ + +	+ + +	+ + +	+	-	+	+	+	n.d.	+	n.d.	IgG2b; k
K-RBD-mAb-33	+ + +	+ + +	+ +	-	-	+	+	+	n.d.	+	n.d.	IgG1; k
K-RBD-mAb-36	+ + +	+ + +	+ +	+ +	+	+	-	+	n.d.	-	-	IgG2a; k
K-RBD-mAb-40	+ + +	+ + +	+ +	+	-	+	+	+	n.d.	+ +	n.d.	IgG1; k
K-RBD-mAb-41	n.d.	+ + +	+	n.d.	n.d.	+	+	+	n.d.	+ +	n.d.	IgG1; k
K-RBD-mAb-42	**+ + +**	**+ + +**	**+ + +**	**+ +**	**+**	**+ +**	**+ +**	**+ +**	**+ +**	**+ +**	**+ + +**	**IgG2a; k**
K-RBD-mAb-43	+ + +	+ + +	+ +	+	-	+	+	+	n.d.	+ +	n.d.	IgG2b; k
K-RBD-mAb-45	+ + +	+ + +	+ + +	+	-	+	+	+	n.d.	+	n.d.	IgG1; k
K-RBD-mAb-53	n.d.	+ + +	+ + +	n.d.	n.d.	+	-	+	n.d.	-	n.d.	IgG2a; k
K-RBD-mAb-54	+ + +	+ + +	+ +	+	-	+	+	+	n.d.	+ +	n.d.	IgG2b; k

(*continued on next page*)

Table 1 (*continued*)

	ELISA Binding Activities*					Neutralizing Activities**						
K-RBD-mAb-56	+ + +	+ + +	+ +	+	-	+	+	+	n.d.	+ +	n.d.	IgG2b; k
K-RBD-mAb-57	+ + +	+ + +	+ +	+ +	+ +	+	+	+	n.d.	+	-	IgG1; k
K-RBD-mAb-60	**+ + +**	**+ + +**	**+ + +**	**+ + +**	**+ +**	**+ +**	**+ + +**	**+ + +**	**+ +**	**+ +**	**+ + +**	**IgG2a; k**
K-RBD-mAb-62	**n.d.**	**+ + +**	**+**	**+ + +**	**+ +**	**+**	**+ +**	**+ +**	**+ +**	**+ + +**	**+ + +**	**IgG2a; k**
K-RBD-mAb-63	-	+	-	-	-	n.d.	n.d.	n.d.	n.d.	n.d.	n.d.	IgG1; k
K-RBD-mAb-67	+ +	+ + +	-	-	-	n.d.	n.d.	n.d.	n.d.	n.d.	n.d.	IgG1; k
K-RBD-mAb-68	+ + +	+	-	-	-	n.d.	n.d.	n.d.	n.d.	n.d.	n.d.	IgG1; k
K-RBD-mAb-71	+ + +	+ + +	+ + +	+	-	+	+	+	n.d.	+	n.d.	IgG2b; k
K-RBD-mAb-73	+ +	+ + +	+ +	+	-	-	-	-	n.d.	-	n.d.	IgG2a; k
K-RBD-mAb-75	**+ + +**	**+ + +**	**+ + +**	**+ + +**	**+ +**	**+ +**	**+ +**	**+ +**	**+ +**	**+ +**	**+ + +**	**IgG2a; k**
K-RBD-mAb-78	+ + +	+ + +	+	-	-	+	+	+	n.d.	-	n.d.	IgG1; k
K-RBD-mAb-79	+	+ + +	-	+	-	n.d.	n.d.	n.d.	n.d.	n.d.	n.d.	IgG2a; k
K-RBD-mAb-80	+ + +	+ + +	+ +	+ +	+	-	-	-	n.d.	-	-	IgG2a; k
K-RBD-mAb-83	n.d.	+ +	+ +	n.d.	n.d.	+	+	+	n.d.	+ +	n.d.	IgG1; k
K-RBD-mAb-85	+ + +	+ + +	+ +	+ +	+	-	-	-	n.d.	-	-	IgG1; k
K-RBD-mAb-88	+ +	+	-	-	-	n.d.	n.d.	n.d.	n.d.	n.d.	n.d.	IgG1; k
K-RBD-mAb-89	+ + +	+ + +	+ +	+	-	+	+	+	n.d.	+	n.d.	IgG1; k
K-RBD-mAb-91	**+ + +**	**+ + +**	**+ + +**	**+ +**	**+**	**+ +**	**+ +**	**+ +**	**+ +**	**+ +**	**+ + +**	**IgG2a; k**
K-RBD-mAb-94	+ + +	+ + +	+ +	+ + +	+	n.d.	n.d.	n.d.	n.d.	+	-	IgG1; k
K-RBD-mAb-97	+ + +	+ + +	+ +	+ +	+ +	n.d.	n.d.	n.d.	n.d.	-	-	IgG1; k
K-RBD-mAb-98	+ + +	+ + +	+ + +	+ + +	+	n.d.	n.d.	n.d.	n.d.	+	-	IgG1; k
K-RBD-mAb-104	+ + +	+ + +	+ +	+	-	n.d.	n.d.	n.d.	n.d.	-	n.d.	IgG1; k
K-RBD-mAb-106	+ + +	+ + +	+ + +	+ + +	+	n.d.	n.d.	n.d.	n.d.	-	-	IgG1; k

(*continued on next page*)

Table 1 (*continued*)

	ELISA Binding Activities*					Neutralizing Activities**						
K-RBD-mAb-111	+ + +	+ + +	+ + +	+ + +	+ +	n.d.	n.d.	n.d.	n.d.	-	-	IgG1; k
K-RBD-mAb-113	+ + +	+ + +	+ + +	+ +	+	n.d.	n.d.	n.d.	n.d.	-	-	IgG1; k
K-RBD-mAb-114	+ + +	+ + +	+ + +	+ +	+	n.d.	n.d.	n.d.	n.d.	-	-	IgG1; k
K-RBD-mAb-115	+ + +	+ + +	+ + +	+ + +	+ + +	n.d.	n.d.	n.d.	n.d.	-	-	IgG1; k
K-RBD-mAb-118	+ + +	+ + +	+ + +	+	-	n.d.	n.d.	n.d.	n.d.	-	n.d.	IgG1; k
K-RBD-mAb-119	+ + +	+ + +	+ + +	+ +	+	n.d.	n.d.	n.d.	n.d.	-	-	IgG1; k
K-RBD-mAb-120	+ + +	+ + +	+ + +	+ +	+	n.d.	n.d.	n.d.	n.d.	-	-	IgG1; k
K-RBD-mAb-122	+ + +	+ + +	+ + +	+ +	+ +	n.d.	n.d.	n.d.	n.d.	-	-	IgG1; k
K-RBD-mAb-124	+ + +	+ + +	+ + +	+ +	+ +	n.d.	n.d.	n.d.	n.d.	-	-	IgG1; k
K-RBD-mAb-125	+ + +	+ + +	+ + +	+ + +	+ +	n.d.	n.d.	n.d.	n.d.	-	-	IgG2a; k
K-RBD-mAb-126	+ + +	+ + +	+ + +	+	-	n.d.	n.d.	n.d.	n.d.	-	n.d.	IgG1; k
K-RBD-mAb-128	+ + +	+ + +	+ + +	+ +	-	n.d.	n.d.	n.d.	n.d.	-	n.d.	IgG2a; k
K-RBD-mAb-129	+ + +	+ + +	+ + +	+ +	+ +	n.d.	n.d.	n.d.	n.d.	-	-	IgG1; k
K-RBD-mAb-131	+ +	+ + +	+	+	-	n.d.	n.d.	n.d.	n.d.	-	n.d.	IgG1; k
K-RBD-mAb-133	+ +	+ + +	+ +	-	-	n.d.	n.d.	n.d.	n.d.	+ +	n.d.	IgG1; k
K-RBD-mAb-137	+ + +	+ + +	+ + +	+ +	+	n.d.	n.d.	n.d.	n.d.	-	-	IgG2a; k
NMIgG	-	-	-	-	-	-	-	-	-	-	-	

Note: +, positive results; - , negative results; n.d., not determined; ELISA*: OD = 0.25–0.75, +, weak; OD = 0.75–1.5, ++, medium; OD > 1.5, +++, strong.**Neutralizing: +, IC_{50} = 1000–100 ng/ml; ++, IC_{50} = 100–10 ng/ml; +++, IC_{50} < 10 ng/ml.

4.2. Construction and expression of chimeric antibodies (chAbs)

The V_H and V_K gene segments of mAbs were amplified by PCR and introduced via appropriate restriction enzyme sites. The V_H genes were cloned in-frame into a modified expression vector with a signal peptide and human IgG1 constant region. The V_K genes were cloned into a modified expression vector with a signal peptide and human kappa chain constant region. The heavy-chain- and light-chain-encoding plasmids were co-transfected into Expi-293F cells (Thermo Scientific) to produce antibodies. Protein G column chromatography (GE healthcare) was performed to purify chimeric IgGs. After dialysis of eluents with PBS, the antibody concentrations were measured using the bicinchoninicacid (BCA) protein assay (Thermo Scientific).

4.3. Measurement of binding kinetics

Binding kinetic measurements were performed at 25 °C using a Biacore T200 (Cytiva). For all measurements, a buffer consisting of PBS pH 7.4 supplemented with 0.005% (v/v) Surfactant P20 (Cytiva) was used as running buffer. 1 μg/mL K-RBD chAbs were immobilized onto a CM5 sensor chip surface to a level of 250 response units (RUs). Gradient concentrations of SARS-CoV-2 BA.1 or

BA.2 RBD protein (from 8 nM to 0.5 nM with twofold dilution) then flowed over the chip surface at a flow rate of 30 μl/min. Single-cycle kinetics program with a contact time of 180 s and a dissociation time of 600 s. Running buffer was also injected using the same program for background subtraction. After each cycle, the sensor was regenerated with 10mM Gly-HCl (pH 1.5). The affinity was calculated using a 1:1 (Langmuir) binding fit model with BIAevaluation software (Cytiva).

4.4. Antibody humanization

A CDR grafting approach was used to generate the humanized antibody from K-RBD-mAbs. First, the amino acid sequence of the V_H and V_L domains of the mAb were aligned with the human Ig variable domain germline database using the NCBI IgBLAST tool. The IGHV1-46*01 and IGKV1-33*01 sequences were selected as the most similar human Ig sequences of K-RBD-mAb-60. The IGHV1-2*06 and IGKV1-33*01 sequences were selected as the most similar human Ig sequences of K-RBD-mAb-62. The V_H and V_L of the mAb were then respectively grafted onto the V_H and V_L frameworks of the selected human Ig gene. Both genes were synthesized and amplified by PCR using Kapa-Hifi DNA polymerase (Roche). The resulting V_H was cloned into a modified pcDNA5-FRT-Gamma1 expression vector with human IgG_1 constant region. The V_L was cloned into a modified p-Kappa-HuGS expression vector. A homologous 3D structure of the Fab was then built based on a previously described computer modeling method [37]. After analyzing the structure with PyMOL software, we identified the key amino acid residues at which mutations may impact the original conformation of the CDRs. These residues were back-mutated to the corresponding mouse residues.

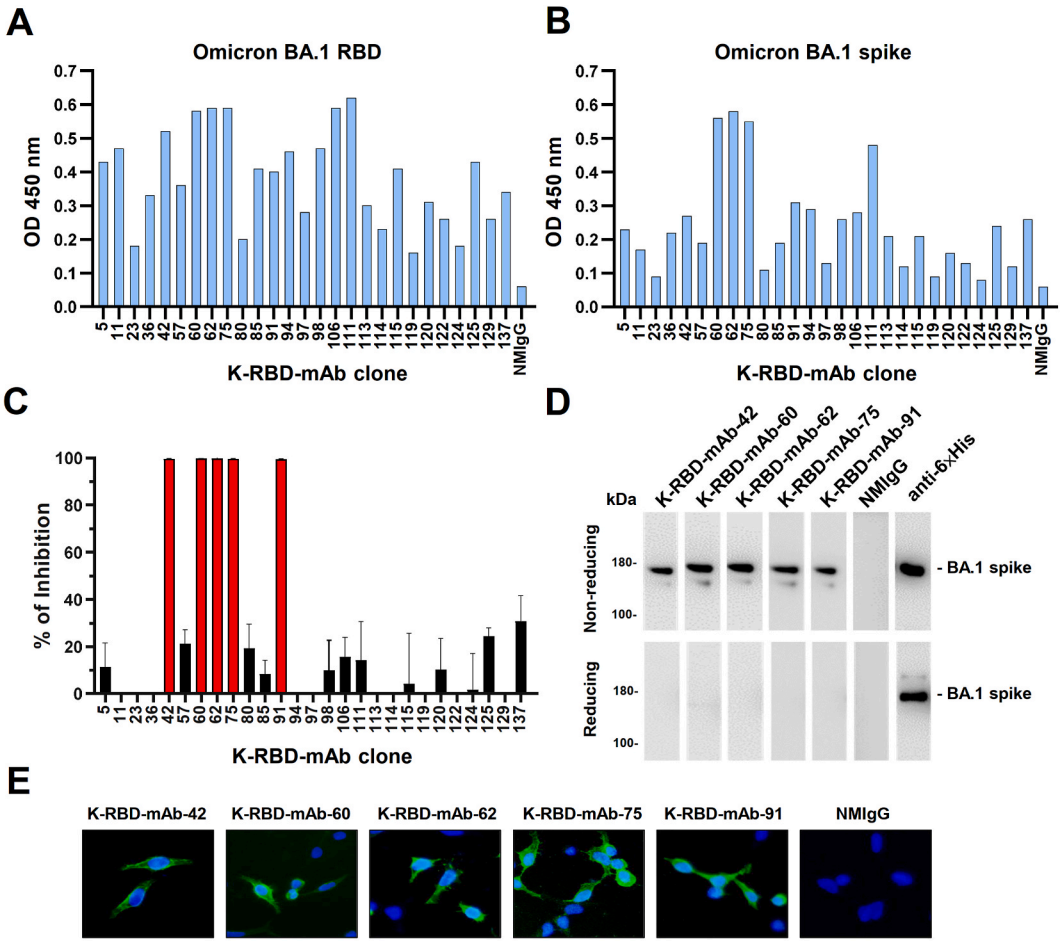

Figure 1. Identification of mAbs targeting the RBD of the Omicron BA.1 variant. Comparative ELISA was performed to assess binding activity of 27 K-RBD-mAbs toward the BA.1 RBD (A) and trimeric BA.1 spike protein (B). ELISA plates were coated with recombinant BA.1 RBD-His and trimeric spike protein (2 μg/mL) and incubated with mAbs that were diluted to 500 ng/mL. Normal mouse IgG (NMIgG) was used as a negative control. (C) Neutralization assay of 27 K-RBD-mAbs (1 μg/mL) for BA.1. Data represent one of two independent experiments. (D) Five K-RBD-mAbs were used as primary antibodies for Western blotting of recombinant BA.1 spike protein-His. Anti-6×His mAb was used as a positive control. Please see Supplemental Figure S1 to find uncropped pictures. (E) BA.1 spike-expressing 293T cells were probed with 1 μg/mL K-RBD-mAbs and then stained with FITC goat anti-mouse IgG. NMIgG was used as a negative control.

4.5. Plaque reduction neutralization test (PRNT)

This assay was performed at the BSL-3 facility in the Institute of Biomedical Sciences, Academia Sinica. The SARS-CoV-2 BA.2 strain was obtained from Taiwan Centers of Disease Control (CDC). Serially diluted hAbs were incubated with 100 PFU SARS-CoV-2 BA.2 for 1 h at 37 °C. Vero E6 cells were added with the virus-hAb mixtures for 1 h adsorption at 37 °C. The viral mixtures were removed and overlaid with DMEM containing 2% FBS and 1% methyl-cellulose. After 4-day incubation, the cells were fixed with 10% formaldehyde overnight and stained with 0.5% crystal violet for 20 min. The plates were washed with tap water, and plaque numbers were counted. Plaque reduction was calculated as: Inhibition percentage = 100 × [1 - (plaque number incubated with mAb/plaque number without mAb)]. The 50% plaque reduction ($PRNT_{50}$) titer was calculated by Prism software.

5. Results

5.1. Generation and identification of mAbs against SARS-CoV-2 spike protein

To generate novel mAbs that bind to SARS-CoV-2 spike protein, we immunized BALB/c mice with LNP-encapsulated mRNAs encoding Kappa spike and RBD. Sixty-one mAbs against Kappa RBD (K-RBD-mAbs) were generated using the mouse hybridoma technique, according to ELISA-based mAb reactivity measurements (Table 1). Most K-RBD-mAbs also recognized the Wuhan and Delta RBDs. Importantly, 27 mAbs in the hybridoma culture supernatants could cross-react with Omicron BA.1 RBD and spike protein. We therefore purified the IgGs of these clones and assessed their binding to Omicron BA.1 RBD and spike (Fig.1A and B). K-RBD-mAb-60, -62, -75 and -111 had the highest binding activities for both target proteins. Next, we further used SARS-CoV-2 spike-pseudotyped lentivirus to screen the neutralizing potentials of the 27 Omicron BA.1-cross-reactive K-RBD-mAbs (Figure 1C). Among the strongest Omicron spike-binding antibodies, K-RBD-mAb-60, -62, and -75, showed high neutralizing activity, whereas K-RBD-mAb-111 did not. In addition, K-RBD-mAb-42 and -91 had only moderate binding activities but exhibited strong neutralizing activities. Of note, the antibody isotypes of the five neutralizing mAbs were IgG2a/kappa (Table 1).

All five Omicron BA.1 neutralizing antibodies (K-RBD-mAb-42, -60, -62, -75 and -91) could recognize recombinant Omicron BA.1 spike protein at its expected molecular weight of 180 kDa in a Western blot analysis under non-reducing conditions (Figure 1D). The

A

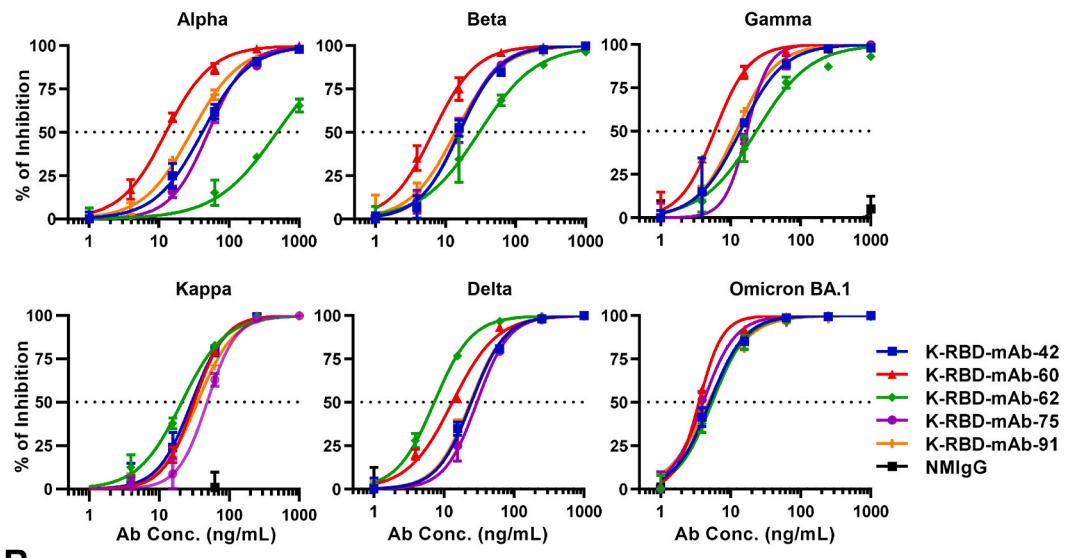

B

Antibody	IC_{50} of Pseudotyped SARS-CoV-2 variants by mAbs (ng/mL)					
	Alpha	Beta	Gamma	Kappa	Delta	Omicron BA.1
K-RBD-mAb-42	43.3 ± 7.3	12.8 ± 2.3	15.4 ± 2.9	35 ± 5.7	25.8 ± 3.6	5.1 ± 0.7
K-RBD-mAb-60	15.7 ± 2.1	6.3 ± 0.9	7.8 ± 1.9	36 ± 4.3	20.6 ± 4.8	3.6 ± 0.3
K-RBD-mAb-62	454.3 ± 16.6	29.2 ± 3.4	33.8 ± 6.3	25 ± 4.1	7.0 ± 0.5	5.8 ± 1.2
K-RBD-mAb-75	50.6 ± 14.2	12.6 ± 1.8	16.0 ± 3.1	62 ± 8.3	38.5 ± 6.9	5.1 ± 1.1
K-RBD-mAb-91	30.5 ± 5.7	12.3 ± 1.1	12.1 ± 2.0	49 ± 3.6	23.2 ± 4.9	7.1 ± 1.4

Figure 2. Neutralizing capacities of K-RBD-mAbs toward SARS-CoV-2 variant pseudoviruses. (A) Dose-response of K-RBD-mAbs in a neutralization assay of SARS-CoV-2 variant pseudovirus. Data are the mean ± SE of three independent experiments. (B) For each antibody, the presented IC50 value was calculated with GraphPad Prism software.

five K-RBD-mAbs could also be used to stain Omicron BA.1 spike protein-expressing 293T cells but not mock-transfected cells, indicating that these mAbs can be applied in immunofluorescence experiments (Figure 1E).

5.2. Neutralizing abilities of K-anti-RBD mAbs

We examined the neutralizing abilities of five K-RBD-mAbs toward SARS-CoV-2 Kappa and five VOCs, including Alpha, Beta, Gamma, Delta and Omicron BA.1 (Figure 2A). Pseudovirus neutralization assays revealed that all five K-RBD-mAbs were capable of neutralizing all six variants, and each mAb exhibited high neutralizing activity toward Omicron BA.1 (IC_{50} values ranged between 3.6 to 7.1 ng/mL; Figure 2B). Among the five mAbs, K-RBD-mAb-62 showed the lowest IC_{50} value (7.0 ng/mL) toward the Delta variant, and K-RBD-mAb-60 exhibited the best neutralizing abilities toward the Alpha, Beta, Gamma and Omicron BA.1 variant. Overall, the K-RBD-mAbs had broad neutralizing activities against SARS-CoV-2 variants, including Omicron BA.1.

5.3. The binding epitopes of K-anti-RBD mAbs

To investigate whether these mAbs share overlapping epitopes, we carried out ELISA-based competition assays (Figure 3A). P44 is a non-neutralizing anti-BA.1 RBD mAb, so it was used as a non-competitor control. We found no positive ELISA signals in competition assays between the five K-RBD-mAbs, suggesting that each mAb fully competes with the others for binding to the RBD. These results suggested that the epitopes for all five mAb mostly overlap. Since the RBD residues, K417, Y453, Q474, F486, Q498, T500 and N501, are the amino acid residues that directly contact ACE2 [38], we sought to clarify whether any of these residues are targeted by the five K-RBD-mAbs. To do so, we mutated each residue to alanine and transiently expressed each mutant in 293T cells. We then performed

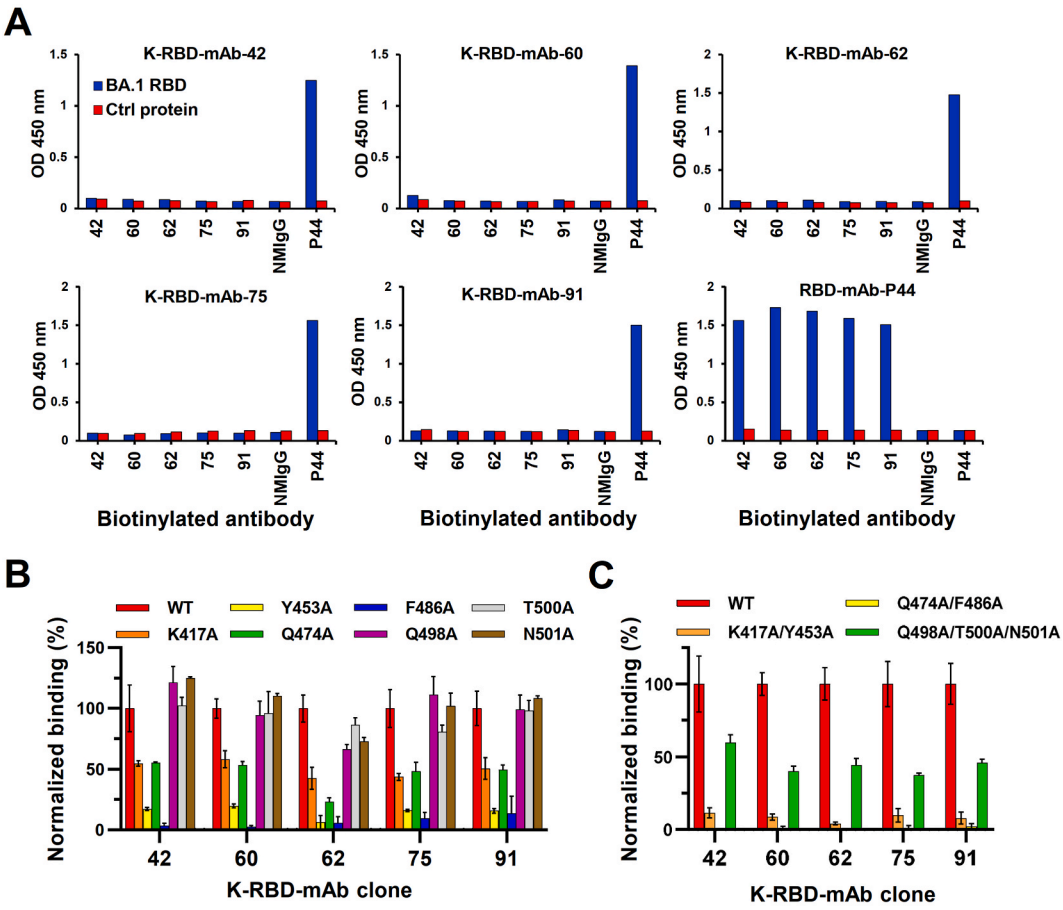

Figure 3. Epitope mapping of neutralizing K-RBD-mAbs. (A) In the ELISA-based epitope competition assay, BA.1 RBD protein was captured by K-RBD-mAb that was immobilized on a 96-well plate. Then, biotinylated antibodies were added to compete for binding of BA.1 RBD. HRP-conjugated streptavidin was added to detect the biotinylated antibodies. Non-competitively binding antibodies produced absorbance signals at OD 450 nm. EpEX-His served as a negative control protein (Ctrl). P44, a non-neutralizing mAb against BA.1 RBD, was used as a positive control. (B–C) Epitope mapping of K-RBD-mAbs according to the mutagenesis assay. 293T cells were made to transiently express wild-type (WT) or mutant RBD proteins with single or multiple alanine mutations. Binding of each mAb to the RBD mutants was examined by cellular ELISA. The results were normalized and are presented as a percent control.

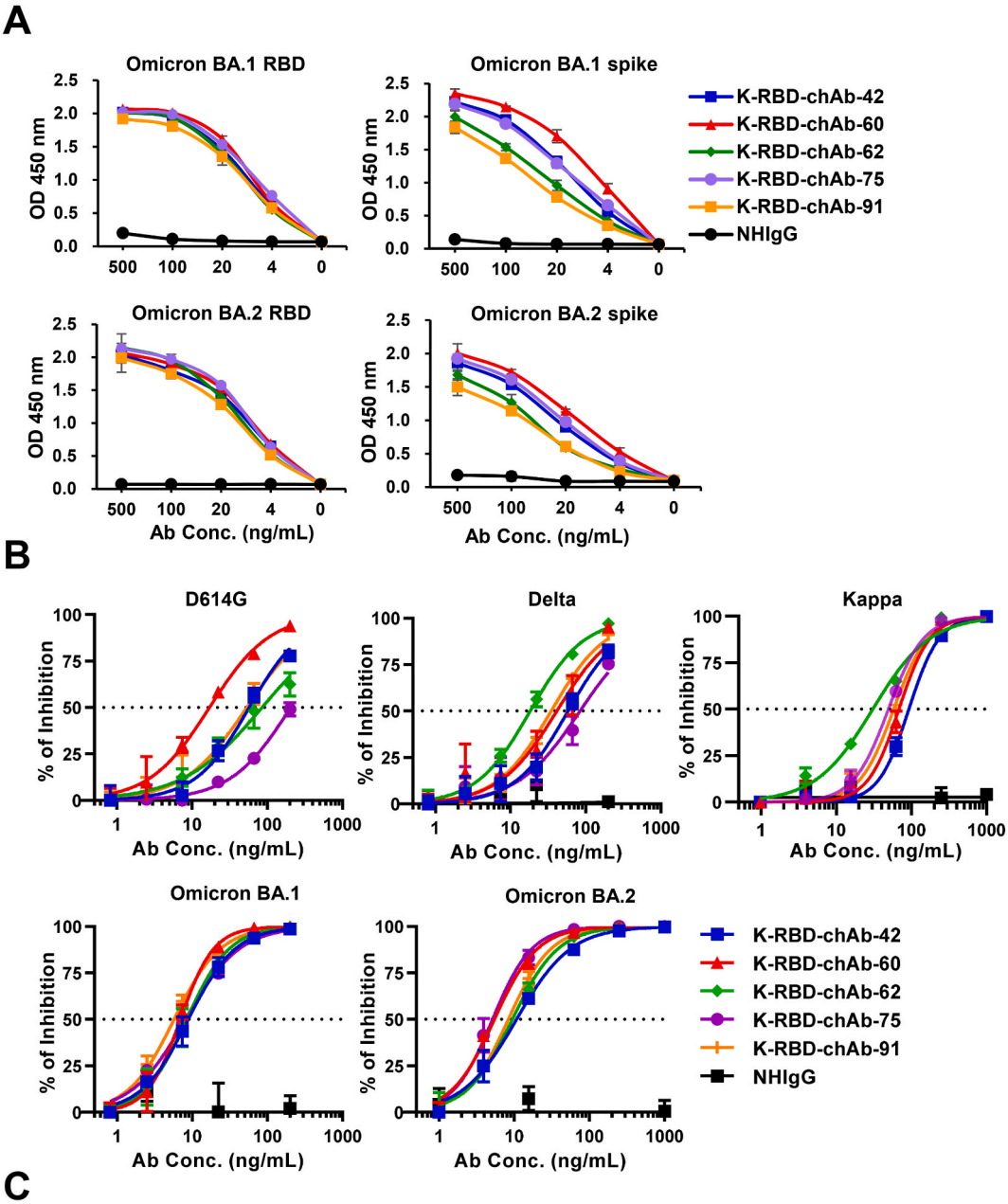

C

Antibody	IC_{50} of Pseudotyped SARS-CoV-2 variants by chAbs (ng/mL)				
	D614G	Kappa	Delta	Omicron BA.1	Omicron BA.2
K-RBD-chAb-42	69.8 ± 8.5	119 ± 7.8	51.2 ± 5.3	8.9 ± 0.5	12.9 ± 2.1
K-RBD-chAb-60	21.5 ± 2.2	72 ± 3.5	49.4 ± 4.1	5.8 ± 0.6	6.3 ± 0.8
K-RBD-chAb-62	105.5 ± 10.1	40 ± 2.8	17.6 ± 0.4	7.8 ± 0.8	9.3 ± 0.2
K-RBD-chAb-75	124.2 ± 42.5	54 ± 3.8	129.6 ± 27.9	10.0 ± 1.1	5.7 ± 0.5
K-RBD-chAb-91	46.6 ± 3.8	64 ± 3.3	46.0 ± 6.7	7.4 ± 1.1	9.5 ± 1.1

Figure 4. Generation of Omicron-neutralizing K-RBD chAbs. (A) ELISA was used to measure binding activity of five K-RBD chAbs to RBD and spike proteins of Omicron BA.1 and BA.2. Serial dilutions were made to evaluate each chAb at 500 to 0 ng/mL. (B) Individual neutralization curves for K-RBD-chAbs were generated based on pseudovirus neutralization assays. Error bars denote the mean ± SE for three technical replicates. (C) For each antibody, the IC50 value was calculated with GraphPad Prism software from three independent experiments, and the values are presented in the table.

alanine scanning by cellular ELISA to test the impacts of each mutation on binding of the K-RBD-mAbs (Figure 3B). The results showed that singleton mutations at Y453 and F486 dramatically decreased the binding of all five mAbs (by more than 80%). The mutation at K417 moderately reduced the binding of the five mAbs. In contrast to the other mAbs, K-RBD-mAb-62 was more sensitive to the Q474 mutation. The combinatorial mutations of K417A/Y453A and Q474A/F486A both substantially disrupted the binding of K-RBD-mAbs (Figure 3C). The combined Q498A/T500A/N501A mutations also had a similar effect on K-RBD-mAbs. Taken together, these data suggest that the RBD epitopes recognized by all five K-RBD-mAbs are very similar.

5.4. Generation of K-RBD chimeric antibodies (chAbs)

To improve the potential of these mAbs for clinical use, we identified the V_H and V_L genes of the five K-RBD mAbs and respectively grafted them onto human IgG1 and kappa backbones to generate K-RBD-chAbs. The ELISA results showed all five K-RBD-chAbs not only bound to the RBD and spike protein of Omicron BA.1 but also to that of BA.2 (Figure 4A). K-RBD-chAb-60 showed the highest binding activities when tested against the BA.1 and BA.2 spike proteins. We next assessed the neutralization profiles of the five K-RBD-chAbs against the variants of SARS-CoV-2 (Figure 4B). The five chAbs exerted substantial neutralizing activities against BA.1 and BA.2 pseudoviruses, with IC_{50} values ranging from 5.7 to 12.9 ng/mL (Figure 4C). Of five chAbs, K-RBD-chAb-60 and -62 exhibited top 2 broad neutralization. Thus, we further analyzed the affinity of the both chAbs toward BA.1 and BA.2 RBD protein using surface plasmon resonance (SPR) assay (Table 2; Supplemental Figure S2). The measured equilibrium constants (K_D) of K-RBD-chAb-60 against BA.1 and BA.2 RBD were 15.1 and 1.44 pM, respectively; the K_D values of K-RBD-chAb-62 against BA.1 and BA.2 RBD were 0.39 and 0.281 nM, respectively.

5.5. Synthesis of humanized therapeutic antibody

K-RBD-chAb-60 showed the broad neutralization activity and the excellent affinity against SARS-CoV-2 variants. The IC_{50} of K-RBD-chAb-62 for Omicron is less than 10 ng/mL, and its IC_{50} values toward Kappa and Delta are the lowest of the five chAbs (Figure 4C). Hence, we chose two chAbs to further develop by synthesizing humanized versions using CDR grafting techniques. The resulting humanized antibodies (hAbs) are named K-RBD-hAb-60 and -62, and their amino acid sequence share >90% identity with human IgG1/Kappa. Since the binding activity of both hAbs against the RBDs of BA.1 and BA.2 appeared to be identical to their chimeric formats (Figure 5A), it is likely that the humanization process did not greatly affect their paratopes. We demonstrated that K-RBD-hAb-60 neutralized BA.1 and BA.2 with respective IC_{50} values of 1.92 and 3.09 ng/mL; IC_{50} values of K-RBD-hAb-62 toward BA.1 and BA.2 were 4.61 and 5.68 ng/mL, respectively (Figure 5B), indicating that the neutralizing activities for BA.1 and BA.2 were retained. However, IC_{50} values of K-RBD-hAb-60 and -62 toward Omicron sublineage BA.5 increased to 1,011 and 464 ng/mL, respectively (Figure 5B). This consistent reduction in neutralization potency for both hAbs might have been due to the F486V mutation in BA.5, as F486 is within the epitopes of our K-RBD-hAbs (Figure 3B). Finally, we performed PRNT assays to investigate the neutralization ability of two K-RBD-hAbs against BA.2 authentic virus (Figure 5C). K-RBD-hAb-60 and -62 each showed potent neutralization activity, with $PRNT_{50}$ values of 1.1 and 1.2 ng/mL, respectively.

6. Discussion

Four major strategies are often used to generate therapeutic mAbs: mouse hybridoma, phage-display Ab library, hAb transgenic mice, and single B cell RT-PCR [15]. The most common approach for rapid isolation of neutralizing antibodies against SARS-CoV-2 has been single cell RT-PCR on memory B cells sorted from *convalescent* or acute-phase COVID-19 patient samples [39, 40]. In addition, the classical mouse hybridoma approach plus further Ab engineering techniques have also contributed to the discovery of neutralizing antibodies during the COVID-19 pandemic [29]. In this study, we used a modified mouse hybridoma technique including mRNA-LNP immunization method to generate mAbs that can broadly neutralize SARS-CoV-2 variant pseudotypes. To the best of our knowledge, only one patent application from Novatis [41] and a study recently published by our group [34] have so far described the use of this efficient method to generate mAbs.

The high number of mutations in the Omicron spike protein have allowed the variant to evade neutralizing antibodies elicited by vaccines and prior natural infections [12, 13]. This immune evasion may be one of the major reasons that Omicron variants have spread so much more quickly than the Wuhan-Hu-1 virus and the Delta variant. Furthermore, nearly all of the therapeutic Abs granted EUAs have been severely compromised by the emergence of Omicron BA.1 [26,27]. For example, bamlanivimab binds the right

Table 2
Kinetic analysis of K-RBD-chAb-60 and -62 against BA.1 and BA.2 RBD protein.

	BA.1 RBD		
Antibody	Ka (1/Ms)	Kd (1/s)	KD (M)
K-RBD-chAb-60	7.48×10^{6}	8.58×10^{-5}	1.51×10^{-11}
K-RBD-chAb-62	9.74×10^{5}	3.8×10^{-4}	3.9×10^{-10}
	BA.2 RBD		
Antibody	Ka (1/Ms)	Kd (1/s)	KD (M)
K-RBD-chAb-60	6.69×10^{7}	9.63×10^{-5}	1.44×10^{-12}
K-RBD-chAb-62	1.74×10^{6}	4.91×10^{-4}	2.81×10^{-10}

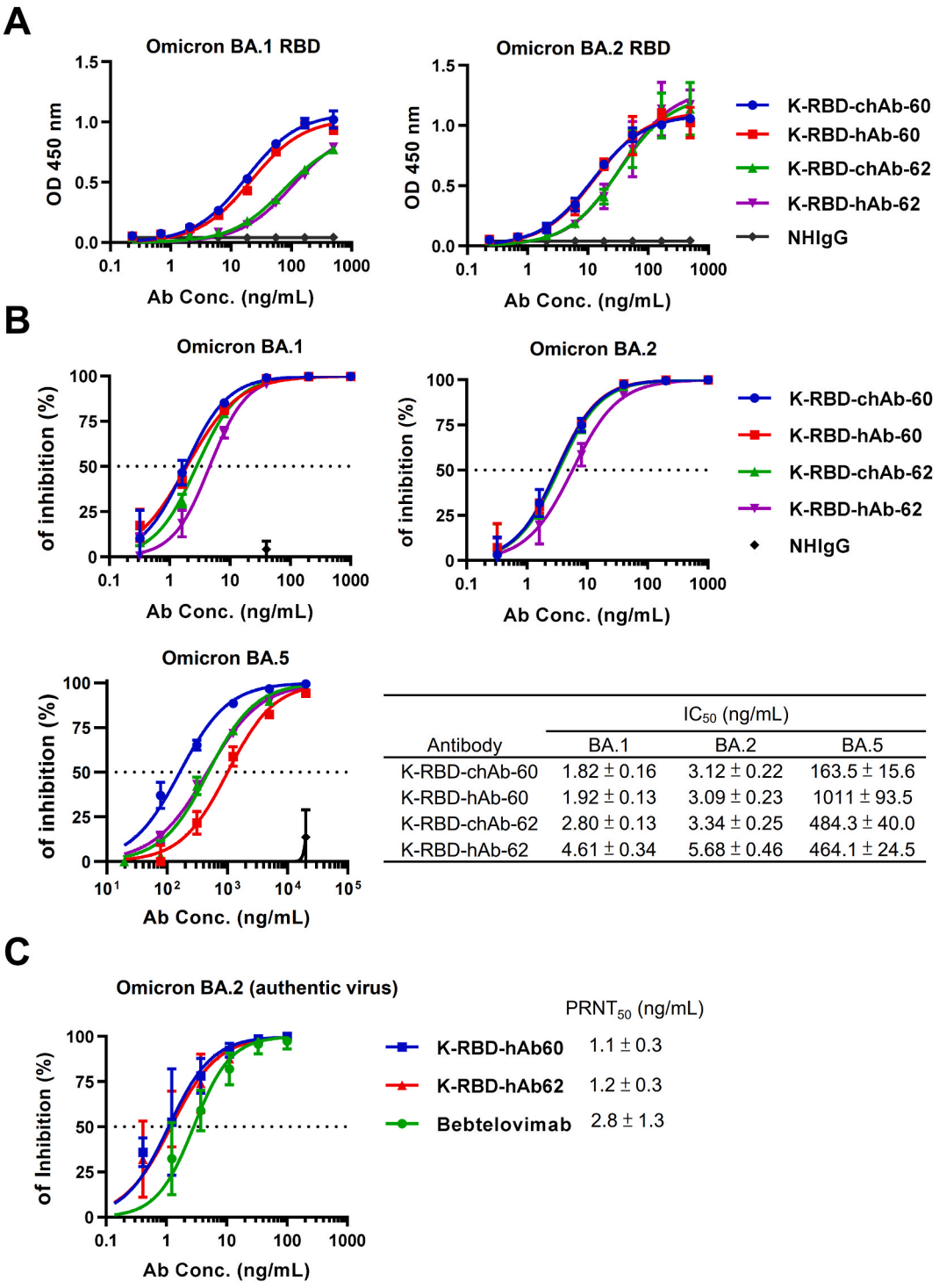

Antibody	IC_{50} (ng/mL)		
	BA.1	BA.2	BA.5
K-RBD-chAb-60	1.82 ± 0.16	3.12 ± 0.22	163.5 ± 15.6
K-RBD-hAb-60	1.92 ± 0.13	3.09 ± 0.23	1011 ± 93.5
K-RBD-chAb-62	2.80 ± 0.13	3.34 ± 0.25	484.3 ± 40.0
K-RBD-hAb-62	4.61 ± 0.34	5.68 ± 0.46	464.1 ± 24.5

Figure 5. Generation of Omicron-neutralizing K-RBD humanized antibody. (A) Omicron binding activities of K-RBD-chAb-60, K-RBD-chAb-62 and their humanized forms were determined by ELISA. (B) Neutralization of Omicron BA.1, BA.2 and BA.5 pseudoviruses by four antibodies. (C) Neutralizing hAb inhibition of SARS-CoV-2 BA.2 infection to Vero E6 cells was assessed by PRNT. The IC50 and PRNT50 values were calculated with Prism software. Each assay was performed in three independent experiments. All data points are shown, along with the mean ± SE.

shoulder of the RBD and is sensitive to changes at E484. Beta, Gamma and Omicron variants all contain mutations at this site and cannot be neutralized by bamlanivimab. The epitopes of etesevimab overlap with the binding site of ACE2, and its binding is reduced by RBD mutations at K417, D420, F456, A475 and L455. Tixagevimab and casirivimab were found to be very sensitive to changes at

F486, N487 and G476 in the RBD, and the multiple mutations S477N/T478K/E484A in Omicron BA.1 significantly decrease the neutralizing activities of these two antibodies. Imdevimab and cilgavimab target the loop-forming residues 440–449 in the RBD; thus, the N440K, G446S, S477N mutations in Omicron BA.1 greatly reduce the neutralization activities of both antibodies. G339 is a part of the sotrovimab epitope, and the G339D mutation in Omicron BA.1 reduces the IC_{50} value of sotrovimab to 200 ng/mL [11]. Here we showed K417, Y453, Q474 and F486 might be common residues in the epitopes of our five neutralizing K-RBD-mAbs (Figure 3B). Interestingly, the K417N, S477N and E484A mutations in Omicron BA.1 and BA.2 are near the putative epitopes of our K-RBD-mAbs, but the mutations did not affect the binding and neutralization activities of these antibodies (Figure 4). In future work, we plan to better define the binding interface of K-RBD-mAbs and Omicron RBD by utilizing cryo-electron microscopy (cryo-EM) analyses.

The BA.2 and BA.1 variants share twelve common mutations in the RBD, while BA.2 has four additional mutations: S371F, T376A, D405N and R408S [42]. In the first half of 2022, the number of BA.2 cases has rapidly increased according to the GISAID database (https://covidcg.org), making it the dominant strain in many countries and suggesting that BA.2 has a selective advantage over BA.1. Using the live-virus focus reduction neutralization test (FRNT), Takashita et al. found that etesevimab and bamlanivimab lost neutralizing activity against BA.2 and BA.1 [46]. Interestingly, imdevimab (REGN10987), retained neutralizing activity against BA.2 (68.7 ng/mL of $FRNT_{50}$), though it was previously shown to have lost neutralizing activity against BA.1. Notably, this report also showed that the $FRNT_{50}$ value for sotrovimab against BA.2 was 1359 ng/mL, which represents a 49.7-fold increase over the value for the wild-type strain [43]. According to new data included in the health care provider fact sheet, the neutralization of BA.2 pseudovirus and authentic virus by sotrovimab was significantly weaker than that of wild-type virus, with a 16-fold reduction in IC_{50} value [44]. The U.S. FDA announced that the authorized dosage of sotrovimab is unlikely to be effective against the BA.2 variant, and the agency updated the EUA to limit sotrovimab use in states where BA.2 is dominant, such as New Jersey and New York [45]. Fortunately, the IC_{50} value of bebtelovimab for BA.2 neutralization was not changed, and this treatment is still expected to be effective against the BA.2 variant [45]. Because of the high mutation rate in the SARS-CoV-2 RNA genome, extensive and continual development of therapeutic antibodies is needed, and combinations of existing neutralizing antibodies should be evaluated for the ability to control new variants of SARS-CoV-2.

The advantages of using mRNA vaccines over traditional protein-based technologies are beginning to be defined. The manufacture of recombinant proteins requires sophisticated technologies and is expensive, resulting in long lead times. Alternatively, mRNA has cost advantages and can be synthesized by a generic process once the nucleic acid sequence is known [31, 46]. mRNA technology also has some advantages related to its mode of *in vivo* protein expression; the use of exogenous mRNA expression can overcome significant barriers to the application of short-lived proteins, but it may have no impact on treatment duration for long-lived proteins [47, 48]. In addition to its remarkable potential as a vaccine substrate, the broad applicability of mRNA technology has been demonstrated in the field of passive immunotherapy (antibody therapeutics) [49]. A previous study showed that single injections of LNP-encapsulated mRNAs encoding heavy chain and light chain can rapidly stimulate expression of anti-rabies and botulinum mAbs *in vitro* and *in vivo*, thereby conferring prophylactic and therapeutic protection in mice [50]. In another study, humanized anti-HER2 Ab (trastuzumab) mRNA was formulated into LNPs for efficient *in vivo* delivery, and the anticancer activity of this treatment was demonstrated [51]. Furthermore, CD5-targeting LNPs were used to deliver mRNA encoding anti-fibroblast activation protein (FAP) chimeric antigen receptor and generate anti-FAP CAR-T cells *in vivo* [52]. The resulting CAR-T cells successfully reduced fibrosis and restored cardiac function after injury. Here, we used our recently established mRNA-LNP-mediated immunization method to generate mAbs against infectious diseases, which may further expand the spectrum of mRNA applications.

In conclusion, we used our mRNA-LNP immunization platform to generate anti-RBD mAbs that bind to and neutralize the five current SARS-CoV-2 VOCs. The engineered K-RBD-chAbs and K-RBD-hAbs neutralized Omicron sublineages BA.1 and BA.2 with low IC_{50} values. Thus, these neutralizing antibodies may be promising tools for controlling current SARS-CoV-2 variants, including Omicron BA.1 and BA.2.

Author contribution statement

Ruei-Min Lu, PhD: Conceived and designed the experiments; Analyzed and interpreted the data; Wrote the paper.
Kang-Hao Liang, PhD: Analyzed and interpreted the data.
Hsiao-Ling Chiang, PhD: Performed the experiments; Analyzed and interpreted the data.
Fu-Fei Hsu, PhD; Hsiu-Ting Lin; Wan-Yu Chen; Feng-Yi Ke, PhD; Monika Kumari, PhD: Performed the experiments.
Yu-Chi Chou, PhD; Yi-Ling Lin, PhD; Mi-Hua Tao, PhD: Contributed reagents, materials, analysis tools or data.
Han-Chung Wu: Conceived and designed the experiments.

Data availability statement

Data included in article/supp. material/referenced in article.

Declaration of interest's statement

The authors declare the following conflict of interests: Related to this work, the Institute of Cellular and Organismic Biology and Biomedical Translation Research Center (BioTReC), Academia Sinica have filed a patent application on which H.C.W., R.M.L., W.Y.C. and H.T.L. are named as inventors. The other authors declare no conflict of interest.

Acknowledgements

We are indebted to the Human Therapeutic Ab R&D Core facility of BioTReC in Academia Sinica, for their assistance with Ab production and analysis. We also thank the National RNAi Core Facility at BioTReC for providing SARS-CoV-2 variant pseudoviruses, and the BSL-3 core facility in IBMS of Academia Sinica for performing PRNT assays.

Abbreviations

COVID-19	Coronavirus disease 2019
SARS-CoV-2	severe acute respiratory syndrome coronavirus 2
RBD	receptor-binding domain
RBM	receptor binding motif
VOC	variant of concern
chAb	chimeric antibody
hAb	humanized antibody
IC_{50}	half maximal inhibitory concentration
EUA	emergency use authorization
FDA	Food and Drug Administration
PRNT	plaque reduction neutralization test

Appendix A. Supplementary data

Supplementary data to this article can be found online at https://doi.org/10.1016/j.heliyon.2023.e15587.

References

[1] C. Cao, Z. Cai, X. Xiao, et al., The architecture of the SARS-CoV-2 RNA genome inside virion, Nat. Commun. 12 (2021) 3917.
[2] A.C. Walls, Y.-J. Park, M.A. Tortorici, A. Wall, A.T. McGuire, D. Veesler, Structure, function, and antigenicity of the SARS-CoV-2 spike glycoprotein, Cell 181 (2020) 281, 92. e6.
[3] W.T. Harvey, A.M. Carabelli, B. Jackson, et al., SARS-CoV-2 variants, spike mutations and immune escape, Nat. Rev. Microbiol. 19 (2021) 409–424.
[4] Y.C. Hwang, R.M. Lu, S.C. Su, et al., Monoclonal antibodies for COVID-19 therapy and SARS-CoV-2 detection, J. Biomed. Sci. 29 (2022) 1. https://doi.org/10.1186/s12929-021-00784-w.
[5] P. Wang, M.S. Nair, L. Liu, et al., Antibody resistance of SARS-CoV-2 variants B. 1.351 and B. 1.1. 7, Nature 593 (2021) 130–135.
[6] N.G. Davies, S. Abbott, R.C. Barnard, et al., Estimated transmissibility and impact of SARS-CoV-2 lineage B.1.1.7 in England, Science 372 (2021) eabg3055.
[7] P. Mlcochova, S.A. Kemp, M.S. Dhar, et al., SARS-CoV-2 B. 1.617. 2 Delta variant replication and immune evasion, Nature 599 (2021) 114–119.
[8] A. Sheikh, J. McMenamin, B. Taylor, C. Robertson, SARS-CoV-2 Delta VOC in Scotland: demographics, risk of hospital admission, and vaccine effectiveness, Lancet 397 (2021) 2461–2462.
[9] C. Jung, D. Kmiec, L. Koepke, et al., Omicron: what makes the latest SARS-CoV-2 variant of concern so concerning? J. Virol. (2022), jvi0207721.
[10] M. Kumari, R.-M. Lu, M.-C. Li, et al., A critical overview of current progress for COVID-19: development of vaccines, antiviral drugs, and therapeutic antibodies, J. Biomed. Sci. 29 (2022) 68. https://doi.org/10.1186/s12929-022-00852-9.
[11] E. Cameroni, J.E. Bowen, L.E. Rosen, et al., Broadly neutralizing antibodies overcome SARS-CoV-2 Omicron antigenic shift, Nature 602 (2022) 664–670.
[12] L. Liu, S. Iketani, Y. Guo, et al., Striking antibody evasion manifested by the Omicron variant of SARS-CoV-2, Nature 602 (2022) 676–681.
[13] D. Planas, N. Saunders, P. Maes, et al., Considerable escape of SARS-CoV-2 Omicron to antibody neutralization, Nature 602 (2022) 671–675.
[14] M. Hoffmann, N. Krüger, S. Schulz, et al., The Omicron variant is highly resistant against antibody-mediated neutralization: implications for control of the COVID-19 pandemic, Cell 185 (2022) 447.
[15] R.M. Lu, Y.C. Hwang, I.J. Liu, et al., Development of therapeutic antibodies for the treatment of diseases, J. Biomed. Sci. 27 (2020) 1. https://doi.org/10.1186/s12929-019-0592-z.
[16] D.M. Weinreich, S. Sivapalasingam, T. Norton, et al., REGEN-COV antibody combination and outcomes in outpatients with covid-19, N. Engl. J. Med. 385 (2021) e81.
[17] M.P. O'Brien, E. Forleo-Neto, B.J. Musser, et al., Subcutaneous REGEN-COV antibody combination to prevent covid-19, N. Engl. J. Med. 385 (2021) 1184–1195.
[18] Y.M. Loo, P.M. McTamney, R.H. Arends, et al., The SARS-CoV-2 monoclonal antibody combination, AZD7442, is protective in non-human primates and has an extended half-life in humans, Sci. Transl. Med. (2022), eabl8124.
[19] R.L. Gottlieb, A. Nirula, P. Chen, et al., Effect of bamlanivimab as monotherapy or in combination with etesevimab on viral load in patients with mild to moderate COVID-19: a randomized clinical trial, JAMA 325 (2021) 632–644.
[20] R. Shi, C. Shan, X. Duan, et al., A human neutralizing antibody targets the receptor-binding site of SARS-CoV-2, Nature 584 (2020) 120–124.
[21] J. Dong, S.J. Zost, A.J. Greaney, et al., Genetic and structural basis for SARS-CoV-2 variant neutralization by a two-antibody cocktail, Nature Microbiol. 6 (2021) 1233–1244.
[22] A. Baum, B.O. Fulton, E. Wloga, et al., Antibody cocktail to SARS-CoV-2 spike protein prevents rapid mutational escape seen with individual antibodies, Science 369 (2020) 1014–1018.
[23] A.L. Cathcart, C. Havenar-Daughton, F.A. Lempp, et al., The Dual Function Monoclonal Antibodies VIR-7831 and VIR-7832 Demonstrate Potent in Vitro and in Vivo Activity against SARS-CoV-2. bioRxiv, 2022, 434607.
[24] K. Westendorf, L. Wang, S. Žentelis, et al., LY-CoV1404 (bebtelovimab) potently neutralizes SARS-CoV-2 variants, bioRxiv (2022).
[25] Y. Cao, J. Wang, F. Jian, et al., Omicron escapes the majority of existing SARS-CoV-2 neutralizing antibodies, Nature 602 (2022) 657–663.
[26] W. Dejnirattisai, J. Huo, D. Zhou, et al., SARS-CoV-2 Omicron-B.1.1.529 leads to widespread escape from neutralizing antibody responses, Cell 185 (2022) 467.
[27] L.A. VanBlargan, J.M. Errico, P.J. Halfmann, et al., An infectious SARS-CoV-2 B.1.1.529 Omicron virus escapes neutralization by therapeutic monoclonal antibodies, Nat. Med. 28 (2022) 6.
[28] E. Takashita, N. Kinoshita, S. Yamayoshi, et al., Efficacy of antibodies and antiviral drugs against covid-19 Omicron variant, N. Engl. J. Med. 386 (2022) 995–998.

[29] S.C. Su, T.J. Yang, P.Y. Yu, et al., Structure-guided antibody cocktail for prevention and treatment of COVID-19, PLoS Pathog. 17 (2021), e1009704.
[30] K.H. Liang, P.Y. Chiang, S.H. Ko, et al., Antibody cocktail effective against variants of SARS-CoV-2, J. Biomed. Sci. 28 (2021) 80.
[31] X. Hou, T. Zaks, R. Langer, Y. Dong, Lipid nanoparticles for mRNA delivery, Nat. Rev. Mater. 6 (2021) 1078–1094.
[32] L.R. Baden, H.M. El Sahly, B. Essink, et al., Efficacy and safety of the mRNA-1273 SARS-CoV-2 vaccine, N. Engl. J. Med. 384 (2021) 14.
[33] F.P. Polack, S.J. Thomas, N. Kitchin, et al., Safety and efficacy of the BNT162b2 mRNA covid-19 vaccine, N. Engl. J. Med. 383 (2020) 2603–2615.
[34] F.-F. Hsu, K.-H. Liang, M. Kumari, et al., An efficient approach for SARS-CoV-2 monoclonal antibody production via modified mRNA-LNP immunization, Int. J. Pharm. 627 (2022), 122256.
[35] R.M. Lu, C.Y. Chiu, I.J. Liu, Y.L. Chang, Y.J. Liu, H.C. Wu, Novel human Ab against vascular endothelial growth factor receptor 2 shows therapeutic potential for leukemia and prostate cancer, Cancer Sci 110 (2019) 3773–3787. https://doi.org/10.1111/cas.14208.
[36] H. Zhou, R.J. Fisher, T.S. Papas, Optimization of primer sequences for mouse scFv repertoire display library construction, Nucleic Acids Res. 22 (1994) 888–889.
[37] A. Waterhouse, M. Bertoni, S. Bienert, et al., SWISS-MODEL: homology modelling of protein structures and complexes, Nucleic Acids Res. 46 (2018) 8.
[38] R. Yan, Y. Zhang, Y. Li, L. Xia, Y. Guo, Q. Zhou, Structural basis for the recognition of SARS-CoV-2 by full-length human ACE2, Science 367 (2020) 1444–1448.
[39] T.F. Rogers, F. Zhao, D. Huang, et al., Isolation of potent SARS-CoV-2 neutralizing antibodies and protection from disease in a small animal model, Science 369 (2020) 956–963.
[40] L. Liu, P. Wang, M.S. Nair, et al., Potent neutralizing antibodies against multiple epitopes on SARS-CoV-2 spike, Nature 584 (2020) 450–456.
[41] J.+3 Dominy, R. Dunn, S. Glaser, M. Keating, C. Klattenhoff, I. Splawski, inventors; NOVARTIS, Assignee. Mrna-Mediated Immunization Methods, 2017. PCT2018 04.08.
[42] J. Yu, A-ry. Collier, M. Rowe, et al., Neutralization of the SARS-CoV-2 Omicron BA.1 and BA.2 variants, N. Engl. J. Med. 386 (2022) 1579–1580, https://doi.org/10.1056/NEJMc2201849.
[43] E. Takashita, N. Kinoshita, S. Yamayoshi, et al., Efficacy of antiviral agents against the SARS-CoV-2 Omicron subvariant BA.2, N. Engl. J. Med. 386 (2022) 1475–1477, https://doi.org/10.1056/NEJMc2201933.
[44] Sotrovimab Fact Sheet for Healthcare Providers, 2022. GlaxoSmithKline, https://www.sotrovimab.com/.).
[45] FDA Updates Sotrovimab Emergency Use Authorization, 2022. U.S. FDA, https://www.fda.gov/drugs/drug-safety-and-availability/fda-updates-sotrovimab-emergency-use-authorization.).
[46] L. Van Hoecke, K. Roose, How mRNA therapeutics are entering the monoclonal antibody field, J. Transl. Med. 17 (2019) 54.
[47] K. Karikó, H. Muramatsu, J.M. Keller, D. Weissman, Increased erythropoiesis in mice injected with submicrogram quantities of pseudouridine-containing mRNA encoding erythropoietin, Mol. Ther. 20 (2012) 948–953.
[48] A. Thess, S. Grund, B.L. Mui, et al., Sequence-engineered mRNA without chemical nucleoside modifications enables an effective protein therapy in large animals, Mol. Ther. 23 (2015) 1456–1464.
[49] T. Schlake, A. Thess, M. Thran, I. Jordan, mRNA as novel technology for passive immunotherapy, Cell. Mol. Life Sci. 76 (2019) 301–328.
[50] M. Thran, J. Mukherjee, M. Pönisch, et al., mRNA mediates passive vaccination against infectious agents, toxins, and tumors, EMBO Mol. Med. 9 (2017) 1434–1447.
[51] Y. Rybakova, P.S. Kowalski, Y. Huang, et al., mRNA delivery for therapeutic anti-HER2 antibody expression in vivo, Mol. Ther. 27 (2019) 1415–1423.
[52] J.G. Rurik, I. Tombácz, A. Yadegari, et al., CAR T cells produced in vivo to treat cardiac injury, Science 375 (2022) 91–96.